PHYSICAL REVIEW C **69**, 031605(R) (2004)

Isospin effects on two-particle correlation functions in $E/A=61$ MeV ^{36}Ar+^{112,124}Sn reactions

R. Ghetti,* V. Avdeichikov,† B. Jakobsson, and P. Golubev
Department of Physics, Lund University, Box 118, S-22100 Lund, Sweden

J. Helgesson
School of Technology and Society, Malmö University, S-205 06 Malmö, Sweden

N. Colonna and G. Tagliente
INFN and Dipartimento di Fisica, Via Amendola 173, I-70126 Bari, Italy

H. W. Wilschut, S. Kopecky,‡ and V. L. Kravchuk
Kernfysisch Versneller Instituut, Zernikelaan 25, NL-9747 AA Groningen, The Netherlands

E. W. Anderson,§ P. Nadel-Turonski, and L. Westerberg
The Svedberg Laboratory, Box 533, S-75121 Uppsala, Sweden

V. Bellini, M. L. Sperduto, and C. Sutera
Laboratori Nazionali del Sud (INFN), Via S. Sofia 44, I-95123 Catania, Italy

(Received 4 September 2003; published 23 March 2004)

Small-angle, two-particle correlation functions have been measured for ^{36}Ar+^{112,124}Sn collisions at $E/A=61$ MeV. Total momentum gated neutron-proton (*np*) and proton-proton (*pp*) correlations are stronger for the ^{124}Sn target. Some of the correlation functions for particle pairs involving deuterons or tritons (*nd*, *pt*, and *nt*) also show a dependence on the isospin of the emitting source.

DOI: 10.1103/PhysRevC.69.031605 PACS number(s): 25.70.Pq, 21.65.+f

The isospin dependence of the nuclear equation of state (EOS) is probably the most uncertain property of neutron-rich matter. This property is essential for the understanding of extremely asymmetric nuclei and nuclear matter as it may occur in the *r* process of nucleosynthesis or in neutron stars [1]. In order to study the isospin-dependent EOS, heavy ion collisions with isotope separated beam and/or target nuclei can be utilized [2]. In these collisions, excited systems are created with varying degree of proton-neutron asymmetry. A noticeable isospin dependence of the decay mechanism has been predicted [3–7]. Sensitive observables should be pre-equilibrium neutron/proton emission ratio [8], isospin fractionation [9–12], isoscaling in multifragmentation [13], and neutron and proton flows [14].

Recently, the two-nucleon correlation function has been considered as a probe for the density dependence of the nuclear symmetry energy [15,16]. In these theoretical studies with an isospin-dependent transport model (IBUU), it was shown that a stiff EOS causes high momentum neutrons and protons to be emitted almost simultaneously, thereby leading to strong correlations. A soft EOS delays proton emission, which weakens the *np* correlation. In this paper we study experimental two-particle correlation functions for systems similar in size, but with different isospin. This work shows that, indeed, an isospin signal can be derived.

Two-particle correlation functions were measured in $E/A=61$ MeV ^{36}Ar-induced collisions on isotope-separated targets of ^{112}Sn and ^{124}Sn. The experiment was performed at the AGOR Superconducting Cyclotron of KVI (Groningen). The interferometer consisted of 16 CsI(Tl) detectors for light charged particles, mounted at a distance 56–66 cm from the target in the angular range $30° \leqslant \theta \leqslant 114°$, and 32 liquid scintillator neutron detectors, mounted 2.7 m from the target behind the "holes" of the CsI array, in matching positions to provide the *np* interferometer [17]. In this analysis, only data from the angular range $60° \leqslant \theta \leqslant 120°$ are used for neutrons. Finally, 32 phoswich modules from the KVI Forward-Wall were mounted in the angular range $6° \leqslant \theta \leqslant 18°$ to collect information on the centrality of the collision. At least one fragment in the Forward-Wall was always required in our selected events, which biases our data towards midperipheral collisions [18,19]. Energy thresholds for *p*, *d*, and *t* in the CsI (Tl) detectors were 8, 11, and 14 MeV, respectively, and for neutrons in the liquid scintillators 2.0 MeV. Details about the experimental setup and the particle energy determination are given in Refs. [17,19,20].

Figure 1 shows the ratios of the *n*, *p*, *d*, and *t* kinetic energy yields measured in ^{36}Ar+^{124}Sn and ^{36}Ar+^{112}Sn (note the different scale in the figure for *n* as compared to *p*, *d*, and *t*). An equal number of events is sorted for the two Sn targets. The different solid angle coverage of *n* and *p* detectors

*Corresponding author: Department of Physics, Lund University, Sweden. Email address: roberta.ghetti@nuclear.lu.se

†Present address: Joint Institute for Nuclear Research, 141980 Dubna, Russia.

‡Present address: Department of Physics, PB 35 (YFL), University of Jyväskylä, FIN-40014, Finland.

§Present address: Department of Physics and Astronomy, Iowa State University, Ames, Iowa 50011-3160.

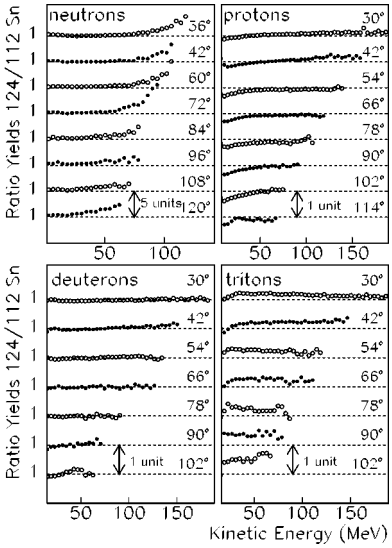

FIG. 1. Ratios of the *n*, *p*, *d*, and *t* kinetic energy yields measured in ^{36}Ar+^{124}Sn and ^{36}Ar+^{112}Sn. The ratios are arbitrarily shifted in the *y* axis (by five units for *n*, by one unit for *p*, *d*, *t*). The dashed lines correspond to unitary ratios (at the angles indicated in the figure).

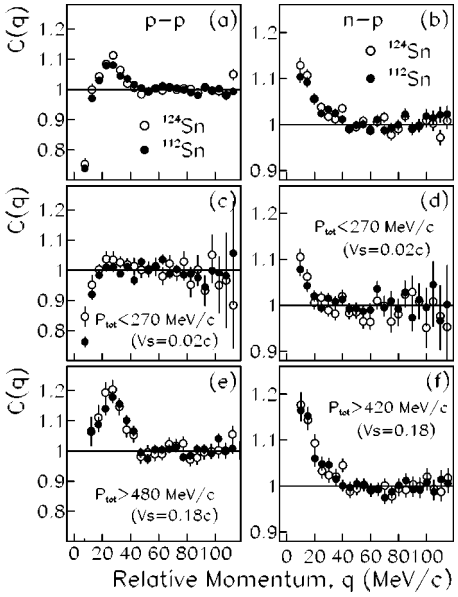

FIG. 2. Angle-integrated ($54° \leqslant \theta \leqslant 114/120°$) *pp* (a,c,e) and *np* (b,d,f) correlation functions from ^{36}Ar+^{112}Sn (filled circles) and ^{36}Ar+^{124}Sn (open circles). Low-P_{tot} (c,d) and high-P_{tot} gated (e,f) correlation functions are also shown.

is accounted for, and the neutron energy is efficiency corrected [17]. One can notice not only a substantial enhancement of the *n* yield for the neutron-rich system (as may be expected), but also that the enhancement is strongly energy dependent. Furthermore, the *p* yield is reduced at low energies for the neutron-rich system and the *t* yield is enhanced over the whole energy range. On the other hand, the yields of the deuteron spectra are the same for the two systems.

The correlation function, $C(\vec{q},\vec{P}_{tot})=kN_c(\vec{q},\vec{P}_{tot})/N_{nc}(\vec{q},\vec{P}_{tot})$, is constructed by dividing the coincidence yield N_c by the yield of uncorrelated events (N_{nc}) constructed from the product of the *singles* distributions [18]. $\vec{q}=\mu(\vec{p}_1/m_1-\vec{p}_2/m_2)$ is the relative momentum, μ is the reduced mass, and $\vec{P}_{tot}=\vec{p}_1+\vec{p}_2$ is the total momentum of the particle pair. The correlation function is normalized to unity at large values of q, $80<q<120$ MeV/c for *pp* and *np* and $160<q<200$ MeV/c for all other particle pairs.

The $54° \leqslant \theta \leqslant 114/120°$ *pp*/*np* correlation functions are presented in Figs. 2(a) and 2(b). The neutron energy threshold is here 8 MeV, to match the proton threshold. The shape of the correlation functions looks as expected from the interplay of quantum statistical and final state interactions. Comparing the two Sn targets, one observes a small but hardly significant enhancement of the correlation strength for ^{124}Sn, in both *pp* and *np* correlation functions.

For the interpretation of the correlation data, it is important to note that the correlation function depends on the space-time extent of the emitting source. From the size of the source, a stronger correlation is expected for the smaller ^{36}Ar+^{112}Sn system, an effect expected also because of the larger excitation energy per particle available for this system (yielding a shorter emission time). On the other hand, the change in neutron number implies a different symmetry energy which also affects the *n* (and *p*) emission times. Neutrons are expected to be emitted faster in the neutron-rich system, which would lead to an enhancement of the correlation strength for ^{36}Ar+^{124}Sn. Thus, the net influence on the correlation function is not easily predictable, both due to the uncertainty in the symmetry energy and to the presence of more than one source of emission.

The emission of light particles from 61*A* MeV (midperipheral) heavy ion reactions originates from (at least) three sources: a projectilelike evaporative source (PLS) and a targetlike evaporative source (TLS) (statistical evaporation) and an intermediate velocity source (IS). The IS represents dynamical emission (DE), which is described by early nucleon-nucleon collisions and by other preequilibrium processes, such as neck emission for noncentral collisions [21–29].

The source analysis of Ref. [30], based on the single-particle energy spectra, has demonstrated that the present data set comprises particles emitted from TLS (source velocity $\sim 0.02c$) and from the IS (source velocity $\sim 0.18c$).[1] Detection of particles emitted from the PLS is instead suppressed, due to the lack of forward angle coverage of our apparatus.

Emission from the different sources can be enhanced/suppressed by introducing cuts in the total momentum of the particle pair, calculated in the relevant emission source frame [18]. It should be remarked that the use of total momentum gates does not guarantee that the selection of the kinematic sources is exclusive, in the sense that contributions from other sources are not excluded. Thus, the event classes contributing to the kinematic regions defined for the figures with total momentum cuts are likely to have some overlap.

[1]The values of the source velocities found in Ref. [30] have been confirmed also by Maxwell-Boltzmann fits to the single-particle energy distributions.

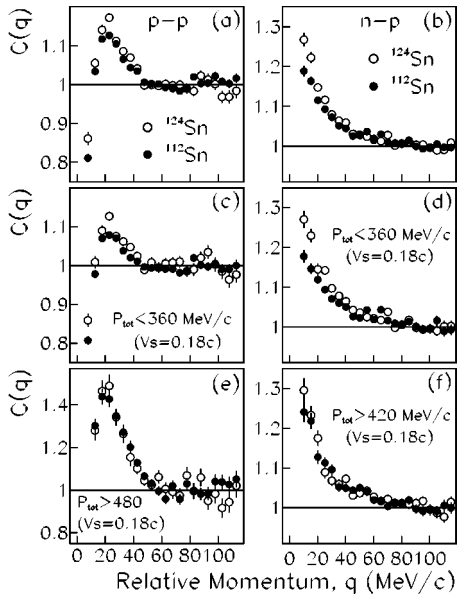

FIG. 3. *pp* correlation functions (a,c,e) measured in the forward detectors $30° \leqslant \theta \leqslant 42°$ and *np* correlation functions (b,d,f) measured in the range $54° \leqslant \theta \leqslant 120°$, with $E_n \geqslant 2$ MeV and $E_p \geqslant 8$ MeV, from ^{36}Ar+^{112}Sn (filled circles) and ^{36}Ar+^{124}Sn (open circles). Low-P_{tot} (c,d) and high-P_{tot} gated (e,f) correlation functions are also shown.

Figures 2(c) and 2(d) present the *pp* and *np* correlation functions for particle pairs with low total momentum (calculated in the reference frame of the TLS), a gate that enhances SE from the TLS. A suppression of the correlation strength is observed, mostly for *pp* and only slightly for the *np* correlation function. This may be expected for particles emitted by SE in the later stages of the collision. Isospin effects are hardly significant for this particle selection.

Figures 2(e) and 2(f) present the *pp* and *np* correlation functions for particle pairs with high total momentum (calculated in the frame of the IS), a gate that may enhance DE from the IS. For both *pp* and *np* correlation functions, an enhancement in the correlation strength is observed relative to the ungated correlation functions. Also in this case, isospin effects are negligible.

Larger isospin effects may be expected if DE emission is enhanced [15,16]. From the kinematics of our collisions, we find that emission from an intermediate velocity source may be enhanced (i) by measuring particle pairs emitted at more forward angles and (ii) by measuring a larger phase-space region at backward angles (low energy particles in lab system). Our experimental setup allows us to apply condition (i) to *pp* pairs and condition (ii) to *np* pairs. Thus, in an attempt to select phase-space regions that favor DE emission, we now look at i) *pp* correlations in the forward $(30° \leqslant \theta \leqslant 42°)$ region (Fig. 3, left column) and ii) *np* correlations that include low energy neutrons ($E_n \geqslant 2$ MeV) in the lab system (Fig. 3, right column). Neutrons with 2–8 MeV energy in the lab system, detected at $60° \leqslant \theta \leqslant 120°$, correspond to 15–45 MeV energy in an IS ($v = 0.18c$) frame. Notice that, for the *np* data, the difference between Figs. 2 and 3 is just the different threshold in the neutron kinetic energy.

Figure 3(a) shows that a stronger *pp* correlation function is now observed for the more neutron-rich system, ^{36}Ar $+^{124}$Sn. To investigate the origin of this enhancement, we apply P_{tot} gates to the *pp* data (calculated in the reference frame of the IS) in an attempt to enhance the earlier and the later stages of DE, respectively, namely, the low-P_{tot} gate in the IS frame should favor later DE, such as preequilibrium neck emission, while the high-P_{tot} gate should favor the earlier preequilibrium emission, such as first chance nucleon-nucleon collisions. Figures 3(c) and 3(e) show that the correlation functions for particle pairs selected by these two complementary gates behave quite differently, indicating that the gate is effectively selecting particles of different origin in the IS frame. The low-P_{tot} gate [~50 % of the yield, Fig. 3(c)] slightly suppresses the correlation function strength, while the high-P_{tot} gate [~25 % of the *pp* yield, Fig. 3(e)] substantially enhances the correlation function strength, as may be expected for proton pairs emitted at the earliest DE times. The isospin signal appears to be associated with the particles selected by the low-P_{tot} gate and to be washed out by the high-P_{tot} gate.

Isospin effects are expected to be more sizable in the *np* correlation function [15]. Indeed, this appears to be the case in our data set. The *np* correlation function at angles 54° −120° (Fig. 3, right column) shows larger isospin effects when the low energy neutrons, $2 \leqslant E_n \leqslant 8$ MeV in the lab system, are included (compare with Fig. 2, right column). The correlation is stronger for the more neutron-rich system, indicating a shorter emission time scale in ^{124}Sn.

To investigate the origin of this isospin effect, we perform the same P_{tot} gates as for *pp* correlations. At backward angles there is a contribution from both the TLS and the IS, but by applying the P_{tot} gates in the IS frame we enhance or suppress the early or late times DE particles (in a background of TLS particles). The results in Figs. 3(d) and 3(f) suggest that the isospin effects seen in Fig. 3(b) come from the late DE particles, and may be attributed to neck emission. In summary, Fig. 3 suggests that the enhancement seen in both *pp* and *np* correlation functions for the neutron-rich system is an isospin effect connected with a faster time scale for particles emitted at the later stages of the DE. This could, for example, be achieved by the density dependence of the nuclear symmetry energy in the neck region [15,16].

Within the multisource reaction mechanism described above, composite particles, such as deuterons and tritons, are believed to be predominantly emitted from the DE source [31,32], where they are formed by a coalescence mechanism [33]. In our data, neither integrated nor P_{tot} gated *dd*, *tt*, and *dt* correlation functions show any appreciable difference between the two Sn targets. This is in agreement with the small sensitivity shown by the calculations of Ref. [34]. Even so, a variation of the correlation functions such as *nd*, *nt*, etc., may be expected, as a consequence of the isospin effects on neutrons and protons. Indeed, this is the case in our experimental data, which can be taken as a further evidence for the presence of true isospin effects. Figures 4(a) and 4(b) present the angle-integrated $(54° \leqslant \theta \leqslant 120°)$ *nd* (a) and *nt* (b) correlation functions, measured for the two Sn targets, with a neutron energy threshold of 2 MeV. The anticorrelation observed for *nd* pairs [Fig. 4(a)] has been observed earlier for

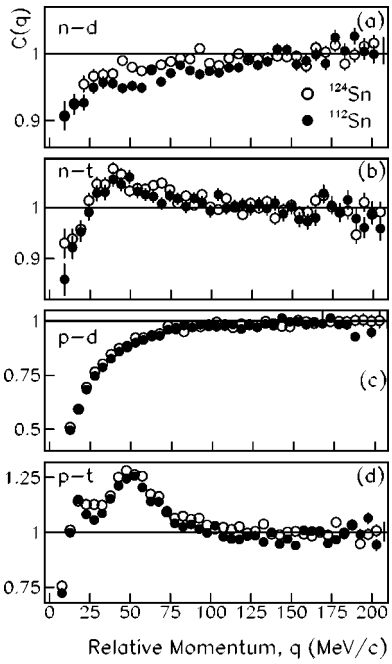

FIG. 4. From ^{36}Ar+^{112}Sn (filled symbols) and ^{36}Ar+^{124}Sn (open symbols): (a,b) *nd*, *nt* ($54° \leqslant \theta \leqslant 120°$); (c,d) *pd*, *pt* ($30° \leqslant \theta \leqslant 42°$).

smaller collision systems, both at lower energies [35] and for 61*A* MeV [19]. It may originate from the depletion of low relative momentum *nd* pairs due to triton formation [36]. In Fig. 4(a) the difference in correlation strength between the two Sn targets can be observed. The fact that a stronger *nd* anticorrelation is found in ^{112}Sn as compared to ^{124}Sn is a puzzling piece of experimental information that certainly deserves theoretical investigation. While it is true that more tritons are formed in ^{124}Sn, it is also true that there are more neutrons in ^{124}Sn, and the actual balance of more *n* (and therefore more *nd* interaction) and more *t* formation (and therefore depletion of *nd* pairs) is not trivial.

The correlation functions of *nt* pairs [Fig. 4(b)] exhibit a broad peak which contains the contributions from the particle-unbound ground state of ^{4}H, and possibly from higher lying excited states [37].[2] Once again, a small enhancement in the strength is observed for the ^{124}Sn target.

The *pd* and *pt* correlation functions, measured in the forward angular range ($30° \leqslant \theta \leqslant 42°$), are shown in Figs. 4(c) and 4(d). The *pd* correlation function (c) is characterized by a pronounced anticorrelation at small *q*, due to final state Coulomb repulsion. The isospin effect is negligible. The *pt* correlation function (d) contains resonance contributions from several excited states of ^{4}He [37]. A small isospin effect is seen in this correlation function.

In summary, isospin effects have been investigated in the $E/A = 61$ MeV ^{36}Ar+^{112}Sn, ^{124}Sn reactions, and, for the first time, correlation functions from systems similar in size but with different isospin have been experimentally determined. Both angle-integrated and total momentum gated correlation functions for all different pairs of particles containing *n*, *p*, *d*, and *t* have been measured. The largest effects from the isospin of the emitting system are seen in the *np* correlation function. In particular, gated *np* correlation functions which should favor a dynamical emission source show a stronger correlation for ^{124}Sn than ^{112}Sn. This could be explained by different time distributions, with a shorter average emission time for the neutron-rich system. Smaller isospin effects are also seen in *pp*, *pt*, *nd*, and *nt* correlation functions. These experimental results demonstrate that two-particle correlation functions indeed provide an additional observable to probe the isospin dependence of the nuclear EOS.

The authors wish to thank S. Brandenburg and the AGOR crew, F. Hanappe, and the DEMON Collaboration. This work was partly supported by the European Commission (Transnational Access Program, Contract No. HPRI-CT-1999-00109) and by the Swedish Research Council (Grant No. F 620-149-2001).

[2]The ground state of ^{4}H should generate a peak at $q \approx 67$ MeV/c, which is not seen in the *nt* correlation function. This may be due to several reasons, including the very broad range of the ^{4}H ground state ($\Gamma_E \approx 5.4$ MeV; $\Gamma_q \approx 57$ MeV/c). However, alternative explanations cannot be excluded until a theoretical investigation of this result has been made.

[1] *Isospin Physics in Heavy-Ion Collisions at Intermediate Energies*, edited by Bao-An Li and W. U. Schröder (Nova Science, New York, 2001).
[2] P. Danielewicz *et al.*, Science **298**, 1592 (2002).
[3] H. Müller and B. Serot, Phys. Rev. C **52**, 2072 (1995).
[4] M. Colonna *et al.*, Phys. Rev. C **57**, 1410 (1998).
[5] Bao-An Li, Phys. Rev. Lett. **85**, 4221 (2000).
[6] Y. G. Ma *et al.*, Phys. Rev. C **60**, 024607 (1999).
[7] J.-Y. Liu *et al.*, Phys. Rev. C **63**, 054612 (2001).
[8] Bao-An Li *et al.*, Phys. Rev. Lett. **78**, 1644 (1997).
[9] V. Baran *et al.*, Nucl. Phys. **A703**, 603 (2002).
[10] Bao-An Li and C. M. Ko, Nucl. Phys. **A618**, 498 (1997).
[11] H. S. Xu *et al.*, Phys. Rev. Lett. **85**, 716 (2000).
[12] W. P. Tan *et al.*, Phys. Rev. C **64**, 051901(R) (2001).
[13] M. B. Tsang *et al.*, Phys. Rev. Lett. **86**, 5023 (2001).
[14] Bao-An Li *et al.*, Phys. Rev. C **64**, 054604 (2001).
[15] L. W. Chen *et al.*, Phys. Rev. Lett. **90**, 162701 (2003).
[16] L. W. Chen *et al.*, Phys. Rev. C **68**, 014605 (2003).
[17] R. Ghetti *et al.*, Nucl. Instrum. Methods Phys. Res. A **516**, 492 (2004).
[18] R. Ghetti *et al.*, Nucl. Phys. **A674**, 277 (2000).
[19] R. Ghetti *et al.*, Phys. Rev. Lett. **91**, 092701 (2003).
[20] V. Avdeichikov *et al.*, Nucl. Instrum. Methods Phys. Res. A **501**, 505 (2003).
[21] C. P. Montoya *et al.*, Phys. Rev. Lett. **73**, 3070 (1994).
[22] J. Tõke *et al.*, Phys. Rev. Lett. **75**, 2920 (1995).
[23] Y. Larochelle *et al.*, Phys. Rev. C **55**, 1869 (1997).
[24] J. Łukasik *et al.*, Phys. Rev. C **55**, 1906 (1997).

[25] P. Pawloswki *et al.*, Phys. Rev. C **57**, 1771 (1998).
[26] Y. Larochelle *et al.*, Phys. Rev. C **59**, R565 (1999).
[27] E. Plagnol *et al.*, Phys. Rev. C **61**, 014606 (1999).
[28] P. M. Milazzo *et al.*, Nucl. Phys. **A703**, 466 (2002).
[29] J. Łukasik *et al.*, Phys. Lett. B **566**, 76 (2003).
[30] V. Avdeichikov *et al.*, Nucl. Phys. A (in press).
[31] G. Lanzanò *et al.*, Nucl. Phys. **A683**, 566 (2001).
[32] T. Lefort *et al.*, Nucl. Phys. **A662**, 397 (2000).
[33] W. J. Llope *et al.*, Phys. Rev. C **52**, 2004 (1995).
[34] L. W. Chen, C. M. Ko, and Bao-An Li, Nucl. Phys. **A729**, 809 (2003).
[35] R. A. Kryger *et al.*, Phys. Rev. Lett. **65**, 2118 (1990).
[36] L. Tomio *et al.*, Phys. Rev. C **35**, 441 (1987).
[37] D. R. Tilley *et al.*, Nucl. Phys. **A541**, 1 (1992).